

## Supporting Information

### **Simultaneous $^1\text{H}$ and $^{13}\text{C}$ NMR enantiodifferentiation from highly resolved pure shift HSQC spectra**

**Míriam Pérez-Trujillo, Laura Castañar, Eva Monteagudo, Lars T. Kuhn, Pau Nolis, Albert Virgili, R. Thomas Williamson, and Teodor Parella\***

## Table of Contents:

### Experimental Section

Figure S1:  $^1\text{H}$  NMR spectrum of racemic compound **1** without and with *R*-PA.

Figure S2: 1D conventional and pure shift  $^1\text{H}$  spectrum of compound **1** and *R*-PA.

Figure S3: Heterodecoupled  $^{13}\text{C}$  NMR spectrum of racemic compound **1** and *R*-PA with expanded multiplets to show individual signal splittings due to the enantiodifferentiation.

Figure S4: Experimental line widths and relative sensitivities obtained in conventional HSQC, pure shift HSQC (psHSQC) and pure shift sensitivity-improved HSQC (psHSQCsi) experiments.

Figure S5: Schematic representation of  $\Delta\Delta\delta(\text{CH})$ .

Figure S6. 2D HSQC and psHSQCsi spectra of racemic compound **1** and *R*-PA.

Figure S7: Expanded area comparing multiplet patterns in SA-HSQC and SAPS-HSQC

Figure S8: Comparison between the conventional coupled  $^{13}\text{C}$ -NMR and SAPS-HSQC experiment in terms of resolution. Evaluation of the effect in  $^{13}\text{C}$  signals when different window functions are applied in the post-processing.

Figure S9: (top) Aliased 2D HSQMBC spectrum of racemic compound **1** and *R*-PA. (bottom) selected 2D cross-peaks corresponding to quaternary carbons.

Figure S10: Experimental  $^{13}\text{C}$  chemical shifts in aliased and conventional HSQC spectra.

Table S1:  $^1\text{H}$  and  $^{13}\text{C}$  NMR chemical shift differences ( $\Delta\Delta\delta(^1\text{H})$  and  $\Delta\Delta\delta(^{13}\text{C})$  in Hz) of racemic compound **1** (2 mM) enantiodifferentiated with *R*-PA (9.6 equiv.) measured from different NMR experiments at 600MHz.

## Experimental Section

NMR experiments were performed on a Bruker Avance 600 spectrometer (Bruker AG, Rheinstetten, Germany) equipped with TXI HCN *z*-grad probes. The temperature for all measurements was set to 298 K and data were acquired and processed with TOPSPIN 3.1 (Bruker AG, Rheinstetten, Germany).

All spectra were recorded on a 600  $\mu$ L fresh solution stock of racemic 3-ethyl-3-(3-hydroxyphenyl)-1-methylazepan-2-one (compound **1**, 29 mM) in CDCl<sub>3</sub>, containing 9.6 equiv. (46.2 mg) of *R*-Pirkle alcohol (PA). It is referred to as compound **1** throughout the manuscript and this SI.

Slice selection in the 1D Zangger-Sterk (ZS) experiment (Fig. 1B) was performed using a selective 180 <sup>1</sup>H R-Snob pulse of 60 ms applied simultaneously to a weak rectangular gradient of 2%. Data was acquired in a pseudo 2D mode using 4 scans for each one of the 16 *t*<sub>1</sub> increments and a recycle delay of 1 s. The FID reconstruction was performed with the AU program pshift (available at <http://nmr.chemistry-manchester.ac.uk>), followed by conventional Fourier transformation. The total experimental time was of 9 minutes.

The 2D <sup>1</sup>H-<sup>13</sup>C pure shift HSQC spectrum (pulse scheme of Fig. 2A) was recorded as described in ref. 6. Pulse phases are *x* unless indicated otherwise and a basic two-step phase cycling scheme is applied:  $\Phi_1=x,-x$ ,  $\Phi_2=x,-x$ . <sup>13</sup>C 180° pulses are applied as CHIRP inversion and refocusing pulses of 500  $\mu$ s and 2000  $\mu$ s of duration, respectively. The recycle delay was 3 s and the interpulse delays in the INEPT and BIRD modules were optimized for 140 Hz ( $\Delta=3.57$  ms). 2 scans were accumulated for each one of the 256 *t*<sub>1</sub> increments (512 experiments defined applying 50% non-uniform sparse sampling), the spectral windows in F1 and F2 dimensions were 377 Hz (2.5 ppm) and 4200 Hz, respectively, the number of data points in *t*<sub>2</sub> was set to 2048 and the acquisition time (AQ) was 0.24 s giving a FID resolution of 1.47 and 4.10 Hz, respectively. The total experimental time was of 30 min. Homodecoupling during acquisition was achieved applying 130 loops (*n*) with  $\tau=7.7$  ms. Broadband heteronuclear decoupling was applied during the  $\tau$  periods using 1.5 ms chirped pulses combined in a p5m4 supercycle scheme. The ratio between the G1:G2 gradients were 40:20.1, measured as percentage of the absolute gradient strength of 53.5 G/cm. Data were acquired and processed using the echo/anti-echo protocol. Sine bell shaped gradients of 1 ms duration were used, followed by a recovery delay of 20  $\mu$ s

( $\delta=1.02\text{ms}$ ). Prior to Fourier-transformation of each data, zero filling to 1024 in F1, 8192 points in F2, linear prediction in F1 and a  $\pi/2$ -shifted sine squared window function in both dimensions were applied. The final digital resolution was of 0.51 and 0.36 Hz in F2 and F1 dimensions, respectively.

To determine  $\Delta\Delta\delta$  on quaternary carbons, a conventional non-refocused gradient-enhanced HSQMBC experiment optimized to 8 Hz was collected with the same acquisition and processing parameters described for the HSQC experiments. 16 scans were acquired per  $t_1$  increment giving a total experimental time of 4 hours. Conventional 2D HSQC experiments were recorded under the same conditions as described previously for the pure shift analogues. HSQC and HSQMBC experiments were also recorded with  $^{13}\text{C}$  spectral windows of 5 ppm (Fig. S6 and S9-10).

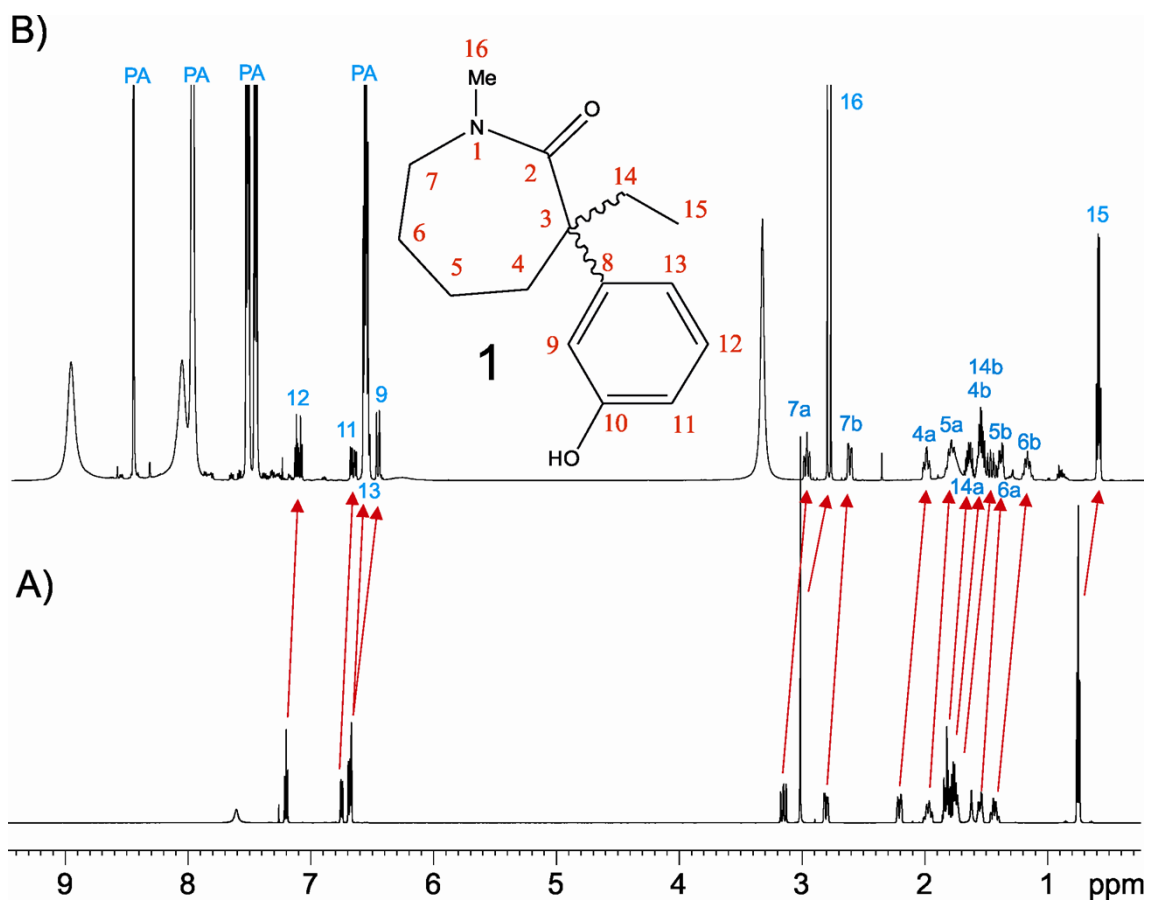


Figure S1: A)  $^1\text{H}$  NMR spectrum of racemic compound (**1**) in  $\text{CDCl}_3$ ; B) Resulting  $^1\text{H}$  NMR spectrum after adding 9.6 equivalents of Pirkle Alcohol (*R*-PA).

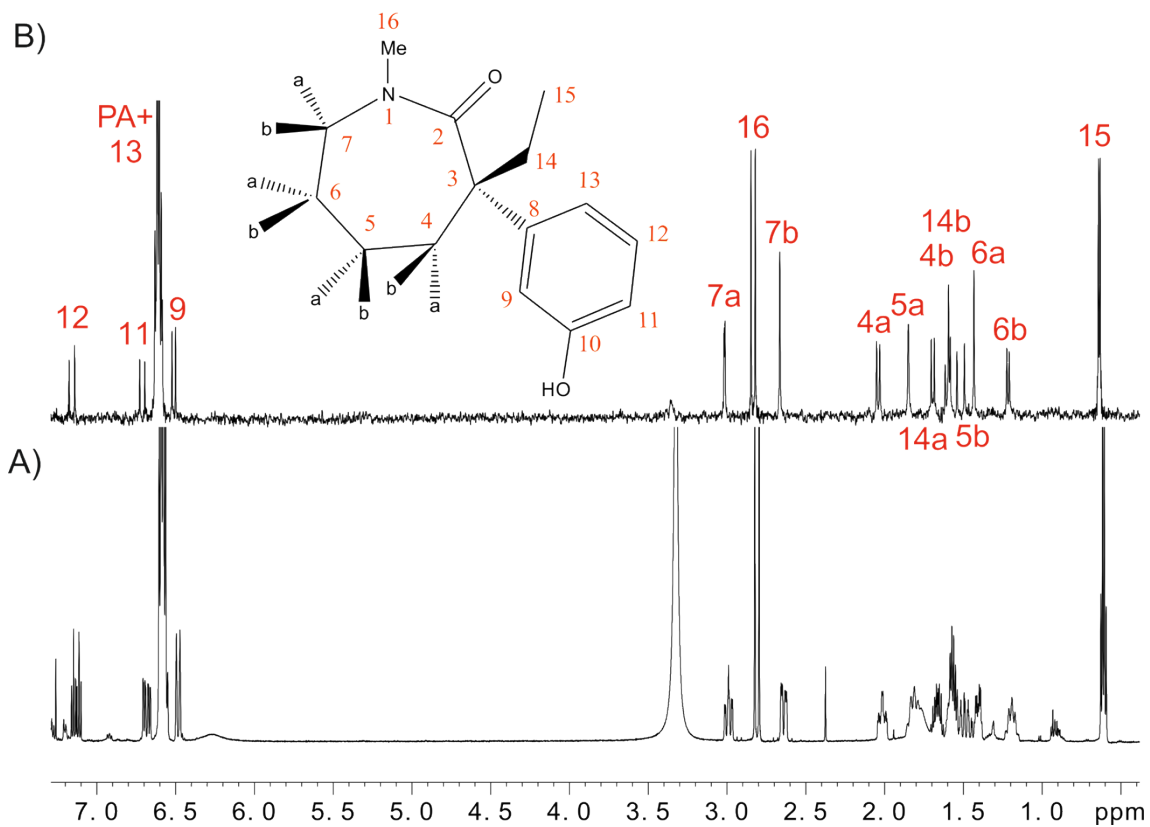


Figure S2: A) 1D conventional and B) pure shift  $^1\text{H}$  spectrum of racemic compound **1** and *R*-PA. The structure of the *R*-1 enantiomer is shown for stereoassignment purposes. See Fig. 1C and 1D for selected expansions and experimental  $\Delta\Delta\delta(^1\text{H})$  values.

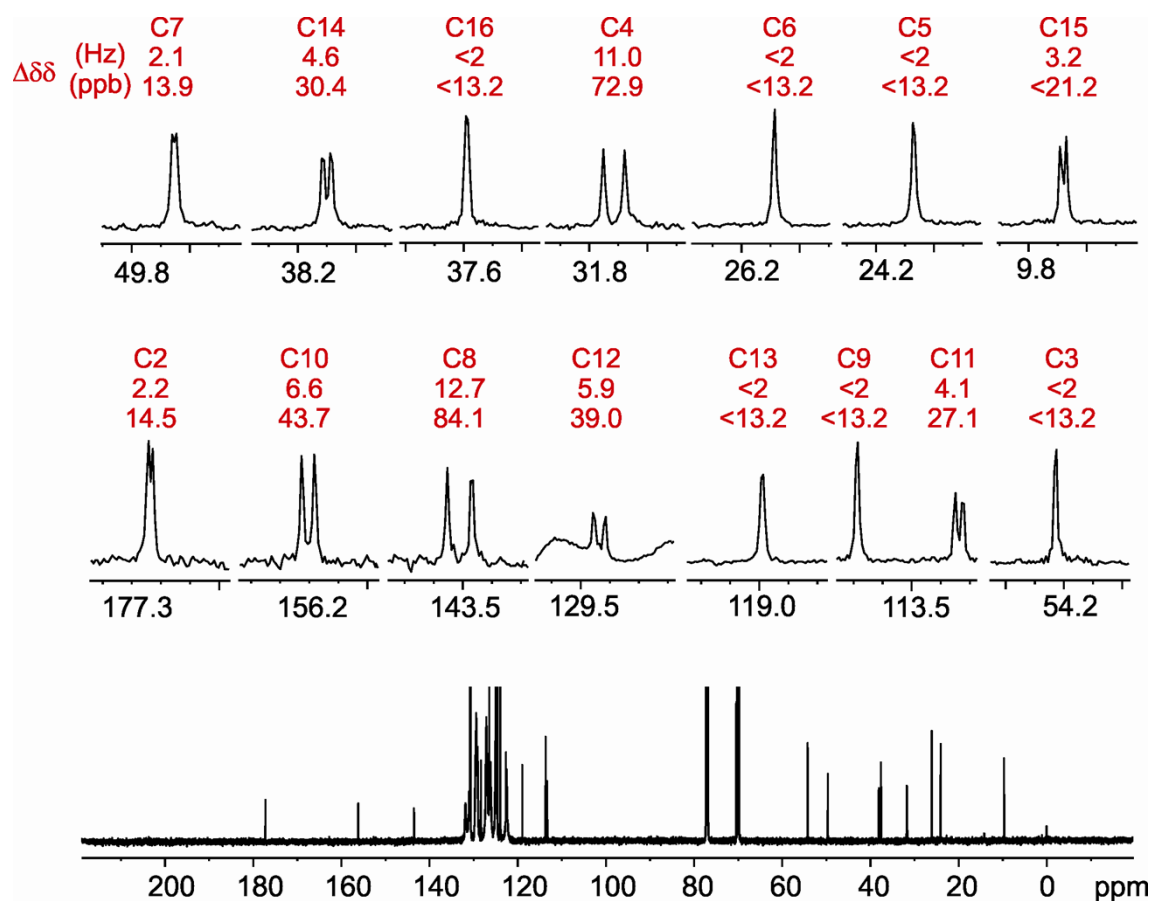


Figure S3: (Bottom) 150.9 MHz Broadband heterodecoupled  $^{13}\text{C}$  NMR spectrum of racemic compound **1** and *R*-PA; (top) expanded multiplets to show individual signal splitting (in Hz and ppb) due to the enantiodifferentiation.

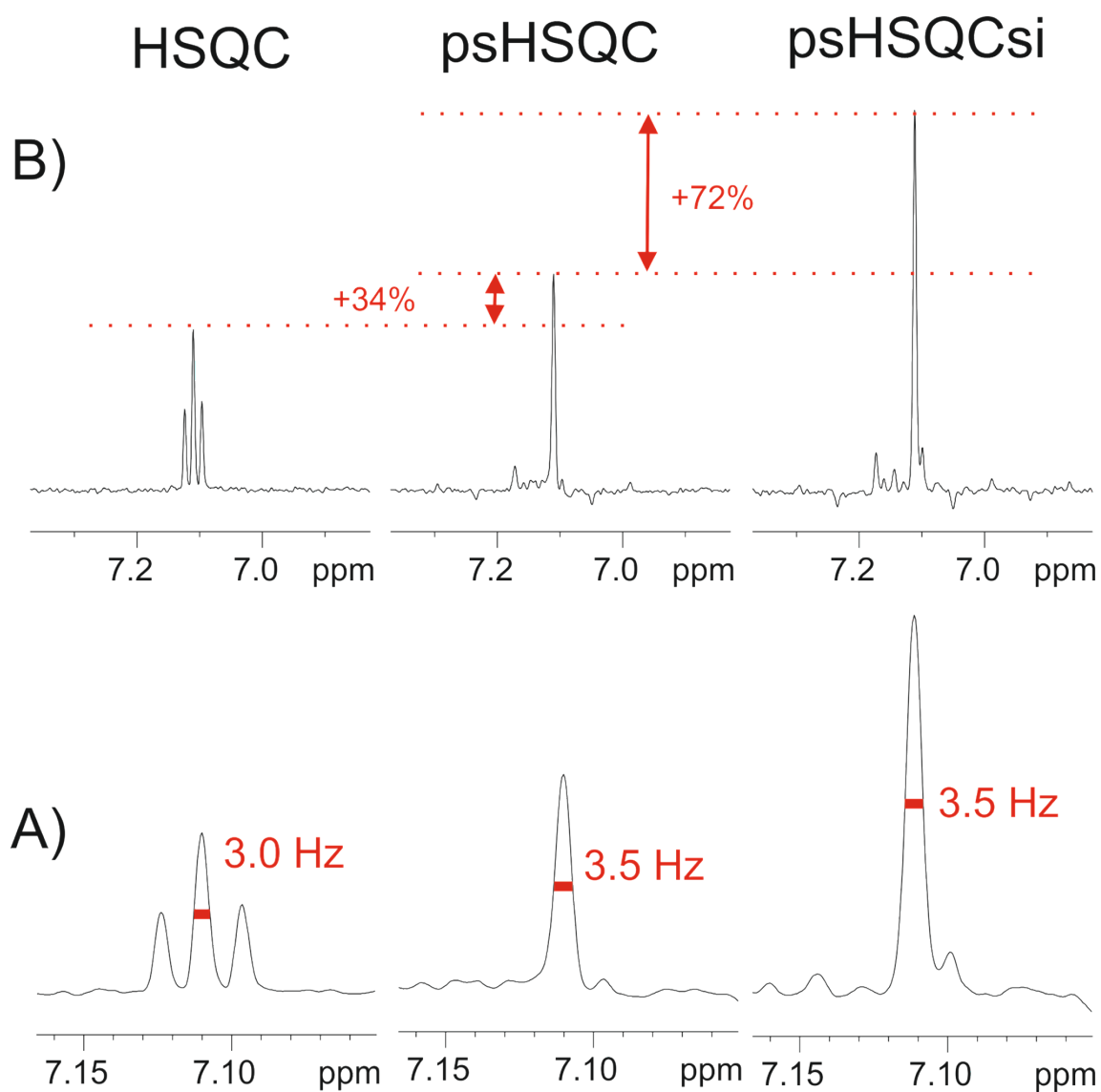


Figure S4: (A) Experimental line widths and B) relative sensitivities obtained in conventional HSQC, pure shift HSQC (psHSQC) and pure shift sensitivity-improved HSQC (psHSQCsi) experiments. 1D traces correspond to the upfield H12/C12 carbon frequency.



$$\Delta\Delta\delta^2(\text{CH}) = \Delta\Delta\delta^2(^1\text{H}) + \Delta\Delta\delta^2(^{13}\text{C})$$

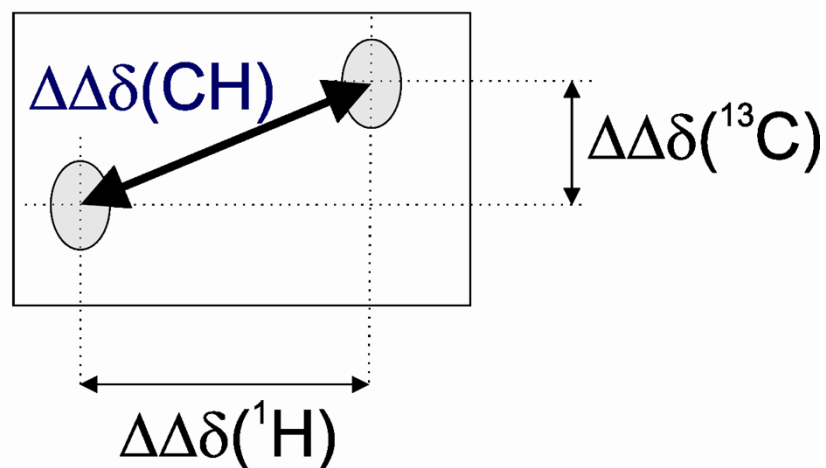


Figure S5: Schematic representation of the new parameter  $\Delta\Delta\delta(\text{CH})$  that defines the separation between two cross-peaks from the individual  $\Delta\Delta\delta(^1\text{H})$  and  $\Delta\Delta\delta(^{13}\text{C})$  separations along each dimension of a 2D map.

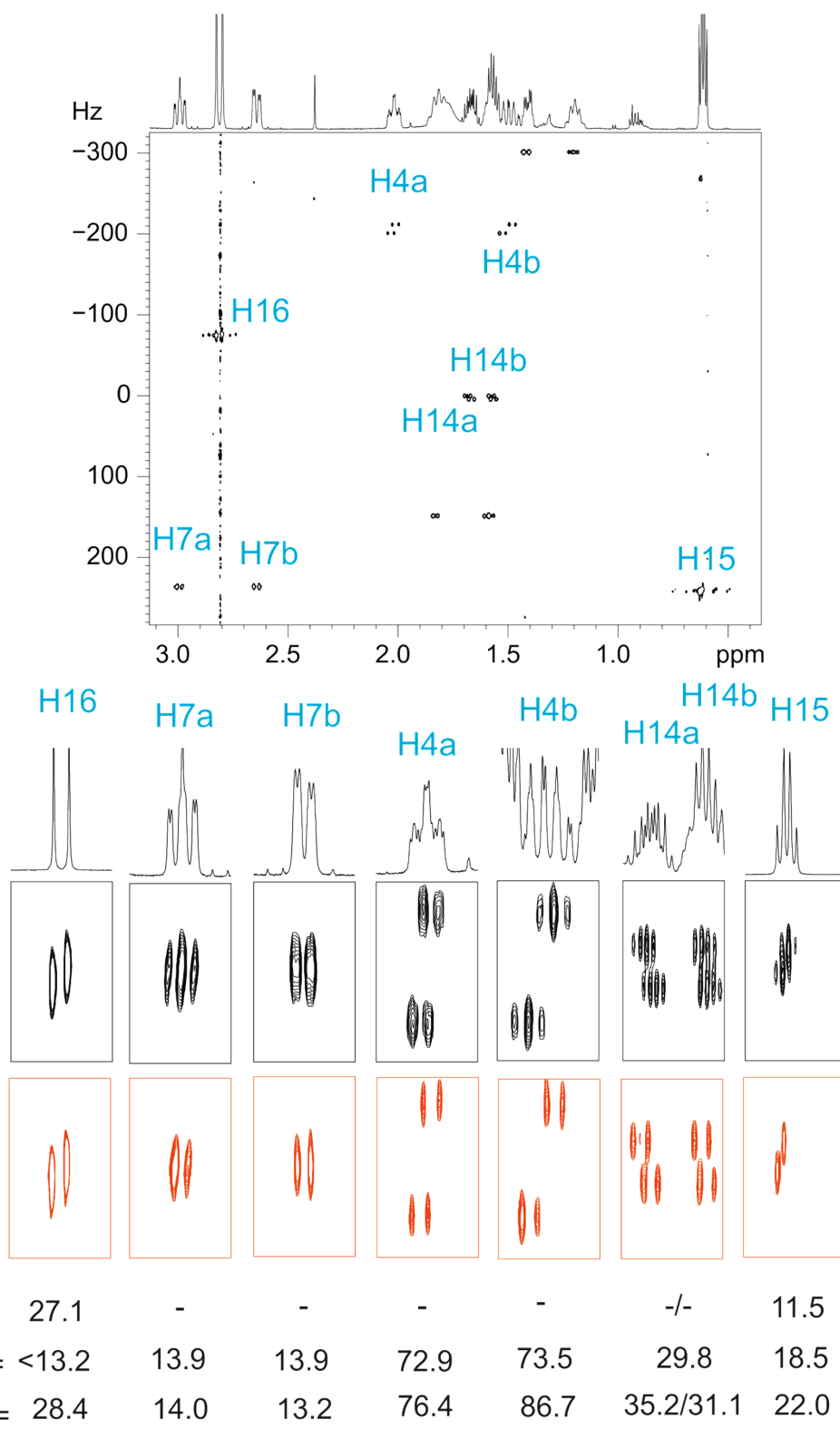


Figure S6: (Top) Expanded area corresponding to the 0.4-3.2 ppm region of the 2D psHSQCsi spectrum of **1** acquired with  $\text{SW}(^{13}\text{C})=5$  ppm; (medium) Expanded cross-peaks show the distinction between enantiomeric signals in 1D  $^1\text{H}$ , conventional HSQC and psHSQCsi spectra; (bottom) experimental values extracted from the conventional  $^1\text{H}$  spectrum ( $\Delta\Delta\delta(^1\text{H})$ ), 1D  $^{13}\text{C}$  spectrum ( $\Delta\Delta\delta(^{13}\text{C})$ ) and calculated ( $\Delta\Delta\delta(\text{CH})$ ) values calculated from the splitting measured in the 2D spectrum.

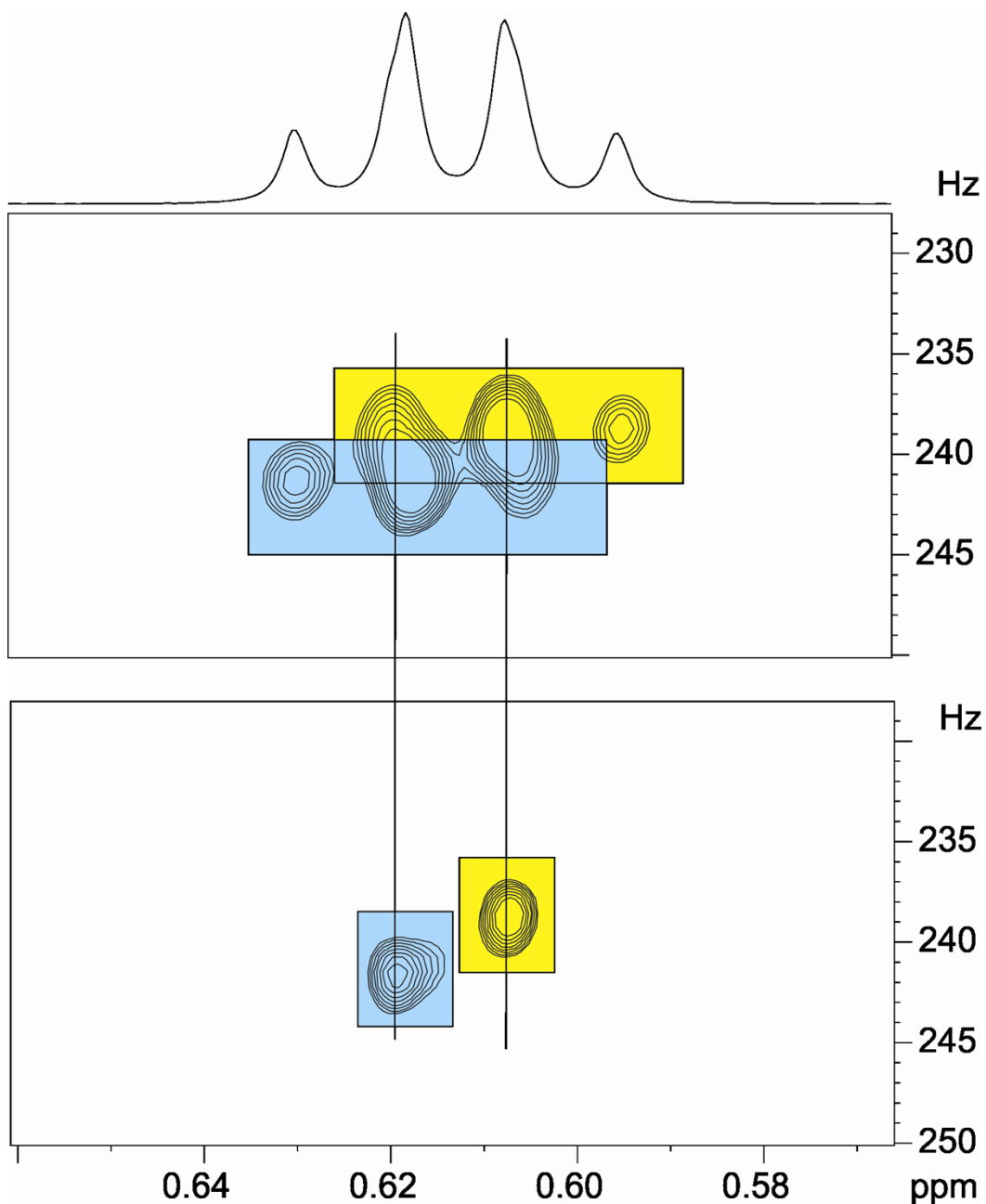


Figure S7: Expanded area corresponding to the C15/H15 cross-peak in (top) SA-HSQC and B) SAPS-HSQC spectra. The H15 signal consists of two overlapped triplets where is difficult to extract the exact  $^1\text{H}$  chemical shift in both  $^1\text{H}$  and conventional HSQC spectra. Note the superior features of the SAPS approach to perform: i) automatic peak picking, ii) accurate and simultaneous determination of  $^1\text{H}$  and  $^{13}\text{C}$  chemical shift differences, and iii) an improved quantification by peak volume integration of each individual singlet signal.

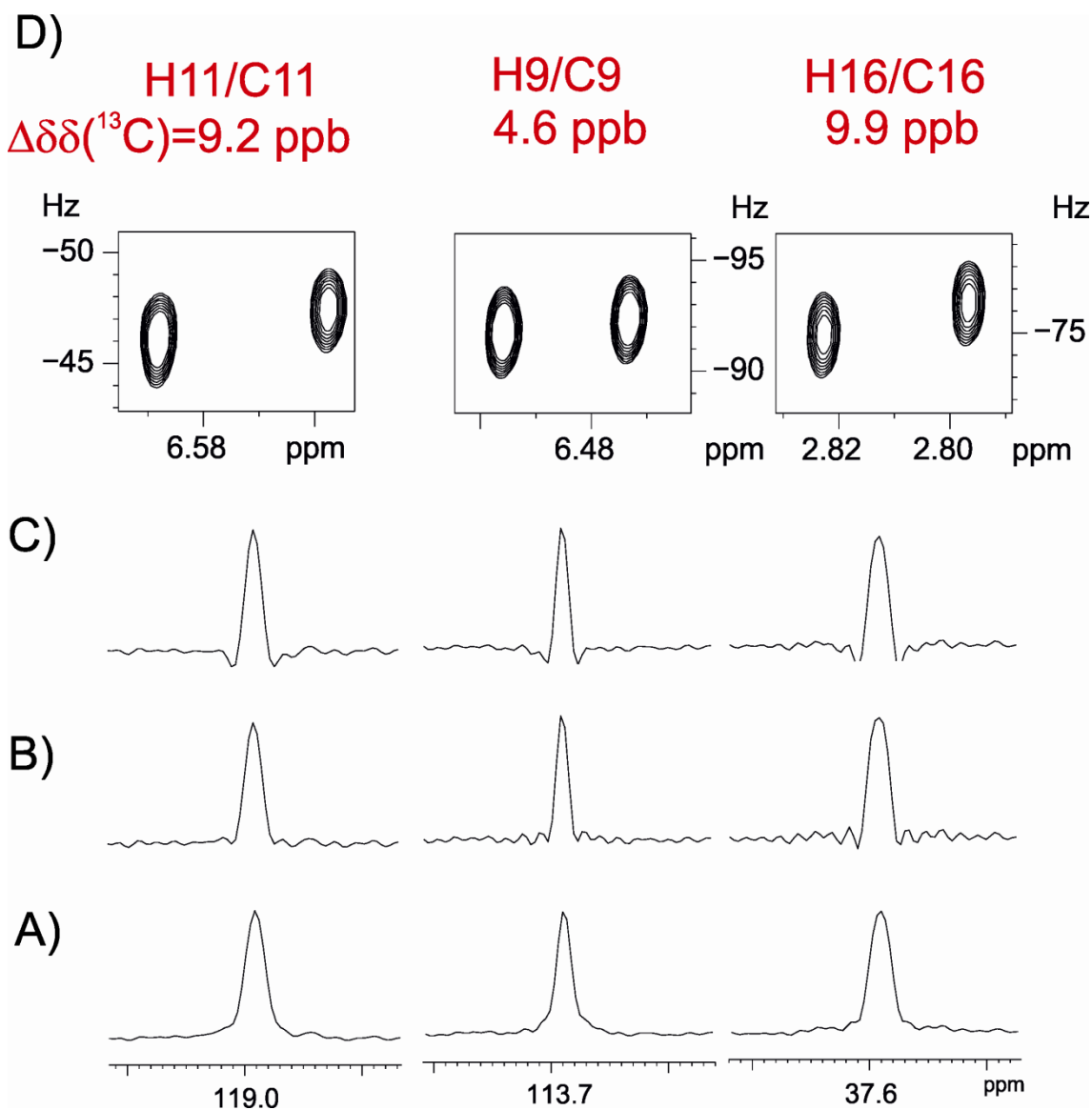


Figure S8: Example showing how the good dispersion along the detected  $^1\text{H}$  dimensions allows the differentiation of small chemical shift differences along the indirect  $^{13}\text{C}$  dimension, even smaller than the line width observed in the conventional  $^{13}\text{C}$  spectrum. A-C) show some not resolved  $^{13}\text{C}$  signals obtained in the conventional  $^{13}\text{C}$  spectrum of 2mM racemic compound 1 complexed with R-PA. Data were acquired with 32K data points and an spectral width of 36057 Hz and further processed with a zero filling up to 64K giving a digital resolution of 0.6 Hz: A) processed with an exponential multiplication with a line broadening of 1 Hz; B) processed without any window function; C) processed with a Gaussian function with LB=-2 Hz and GB=0.5. The line widths at the half of well resolved signals in spectra B was about 1.7 Hz. D) Expansions of the corresponding cross-peaks obtained from the SPS-HSQC spectra.

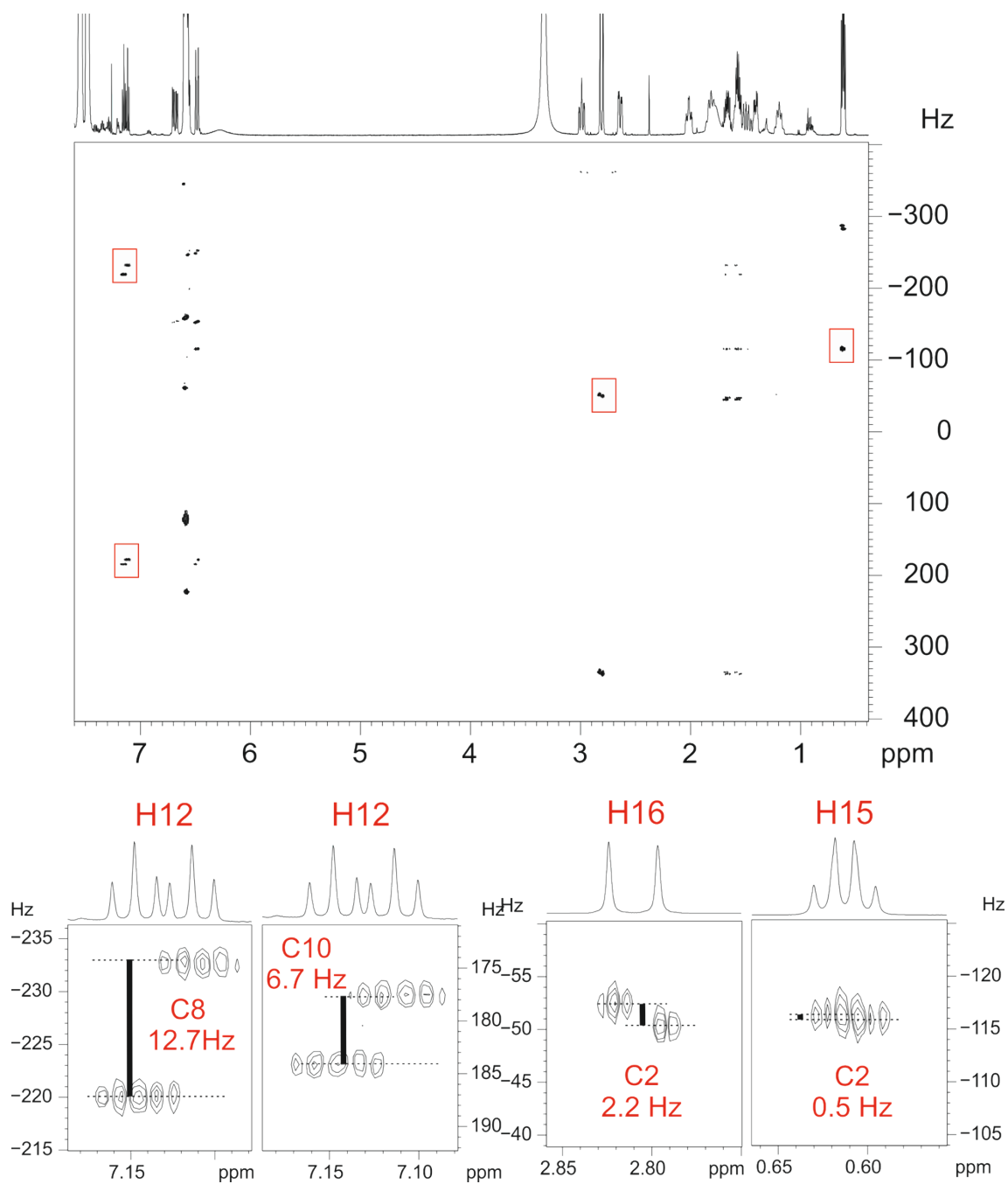
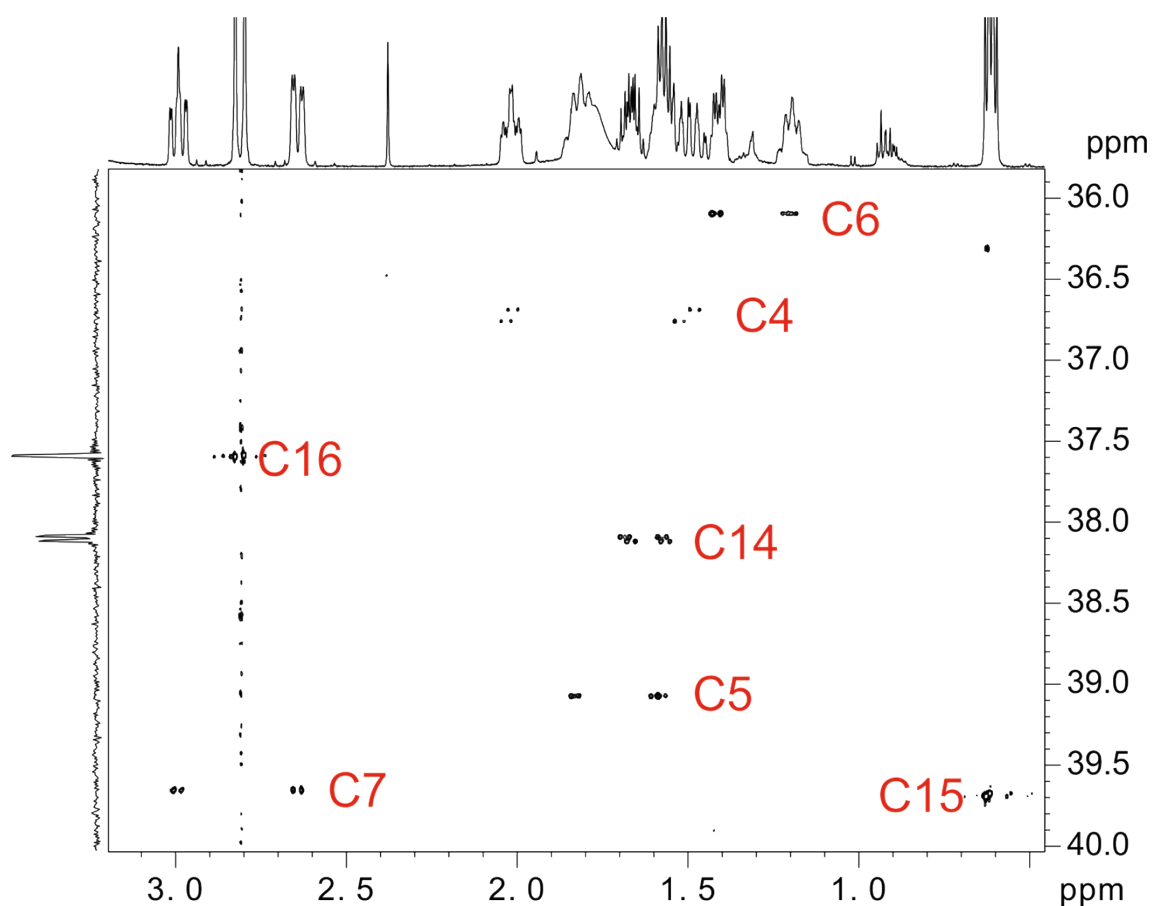


Figure S9: (top) Aliased 2D HSQMBBC spectrum of **1**, acquired with a <sup>13</sup>C spectral width of 5.0 ppm. (bottom) Some selected 2D cross-peaks corresponding to quaternary carbons where  $\Delta\Delta\delta(^{13}\text{C})$  values ranging from 12.7 to 0.5 Hz (84.1 to 3.3 ppb, respectively) can be extracted from the F1 dimension.



Position	$\delta(^{13}\text{C})$		K factor
	Aliased HSQC	HSQC	
C6	36.08	26.08	-2
C4	36.67/36.75	31.67/31.75	-1
C16	37.60	37.60	0
C14	38.08/38.11	38.08/38.11	0
C15	39.06	24.06	-3
C7	39.64/39.65	49.64/49.65	2
C15	39.67/39.69	9.67/9.69	-6

Figure S10: Chemical shifts in aliased and conventional 2D psHSQCsi spectra. Experimental parameters in the indirect dimension: carrier frequency= 38.0 ppm and  $^{13}\text{C}$  spectral width= 5 ppm.

Table S1:  $^1\text{H}$  and  $^{13}\text{C}$  NMR chemical shift differences ( $\Delta\Delta\delta(^1\text{H})$  and  $\Delta\Delta\delta(^{13}\text{C})$  in Hz) of racemic compound **1** (2 mM) enantiodifferentiated with *R*-PA (9.6 equiv.) measured from different NMR experiments at 600MHz.

Position	$\Delta\Delta\delta(^1\text{H})$ [in Hz]			$\Delta\Delta\delta(^{13}\text{C})$ [in Hz]			$\Delta\Delta\delta$ (CH) [in Hz]
	1D $^1\text{H}$	1D ZS- $^1\text{H}$	Pure shift HSQC <sup>c</sup>	1D $^{13}\text{C}$	Pure shift HSQC <sup>c</sup>	HSQMBC <sup>b</sup>	
2	-	-	-	2.2	-	2.2	16.1
3	-	-	-	<2	-	0.5	7.2
4a/4b	x <sup>a</sup> /x <sup>a</sup>	12.0/28.2	12.5/27.7	11.0	11.1	-	16.7/29.8
5a/5b	x <sup>a</sup> /x <sup>a</sup>	<2/ x <sup>a</sup>	1.5/12.6	<2	0.8	-	1.7/12.6
6a/6b	x <sup>a</sup> /x <sup>a</sup>	<2/9.4	<2/10.0	<2	<0.5	-	<1/10.0
7a/7b	x <sup>a</sup> /x <sup>a</sup>	3.5/<2	2.8/0.7	2.1	2.0	-	3.4/2.1
8	-	-	-	12.7	-	12.7	24.3
9	13.5	13.7	14.0	<2	0.7	-	14.0
10	-	-	-	6.6	-	6.7	21.7
11	18.5	19.1	18.4	4.1	3.9	-	18.8
12	20.7	20.9	20.7	5.9	5.8	-	21.4
13	x <sup>a</sup>	x <sup>a</sup>	19.2	<2	1.4	-	19.2
14a/14b	x <sup>a</sup> /x <sup>a</sup>	11.5/ x <sup>a</sup>	11.3/5.9	4.6	4.5	-	12.1/7.4
15	6.9	6.7	7.2	3.2	2.8	-	7.7
16	16.2	16.3	16.0	<2	1.5	-	16.1

<sup>a</sup> Not determined

<sup>b</sup> Only relevant data on quaternary carbons is shown

<sup>c</sup> Digital resolution of  $\pm 0.3$  and  $\pm 0.4$  Hz for  $^1\text{H}$  and  $^{13}\text{C}$  respectively.